



Position sensitive detector at the upgraded LHCf detector

T. SUZUKI¹, O. ADRIANI^{2,3}, L. BONECHI², M. BONGI², G. CASTELLINI^{2,3}, R. D ' ALESSANDRO^{2,3}, K. FUKATSU⁴, M. HAGUENAUER⁵, Y. ITOW^{4,6}, K. KASAHARA¹, K. KAWADE⁴, T. MASE⁴, K. MASUDA⁴, H. MENJO^{2,6}, G. MITSUKA⁴, Y. MURAKI⁴, K. NODA⁷, P. PAPINI², A.-L. PERROT⁸, S. RICCIARINI^{2,9}, T. SAKO^{4,6}, Y. SHIMIZU¹, K. SUZUKI⁴, K. TAKI⁴, T. TAMURA¹⁰, S. TORII¹, A. TRICOMI^{7,11}, W. C. TURNER¹²

¹*Waseda Research Institute for Science and Engineering, Waseda University, Japan*

²*INFN Section of Florence, Italy*

³*University of Florence, Italy*

⁴*Solar-Terrestrial Environment Laboratory, Nagoya University, Nagoya, Japan*

⁵*Ecole-Polytechnique, Palaiseau, France*

⁶*Kobayashi-Maskawa Institute for the Origin of Particles and the Universe, Nagoya University, Nagoya, Japan*

⁷*INFN Section of Catania, Italy*

⁸*CERN, Switzerland*

⁹*Centro Siciliano di Fisica Nucleare e Struttura della Materia, Catania, Italy*

¹⁰*Kanagawa University, Japan*

¹¹*University of Catania, Italy*

¹²*LBL, Berkeley, California, USA*

taku-1984@akane.waseda.jp

DOI: 10.7529/ICRC2011/V05/0264

Abstract: The LHC forward (LHCf) experiment is an experiment to measure the neutral particles emitted in the very forward region of the collision point of LHC. Its goal is to provide data to discriminate the various hadronic interaction models used in cosmic-ray physics. The first phase of the experiment has been achieved on July 2010 with center-of-mass energy $\sqrt{s} = 7$ TeV, and the first result has been submitted. The data analysis of data is still ongoing. The next phase is planned on 2014 at $\sqrt{s} = 14$ TeV. An upgrade of the detector is necessary to cope with the radiation damage of our plastic scintillator and the position sensitive scintillating fiber (SciFi) due to the higher beam intensity with the higher energy than the 7 TeV case. For this purpose, GSO scintillator, which has a high radiation resistivity, has been chosen. Small scaled GSO scintillators (GSO bars) have been manufactured to construct a position sensitive detector. The detector, GSO bundle, consists of GSO bars in a single hodoscope plane. In this paper, we describe the expected performance of a GSO bar system in order to replace SciFi. For this purpose, we made a single layer hodoscope consisting of several GSO bars and performed tests using low-energy heavy ion (Carbon) beam as well as cosmic ray muons. We discuss mainly the position resolution and the simulated performance when the system is applied to cascade showers.

Keywords: high-energy cosmic-ray, LHC, GSO scintillator, position sensitive detector, hadronic interaction

1 Introduction

The LHCf experiment [1] is one of the six experiments of LHC (Large Hadron Collider), and is dedicated for cosmic ray physics. The aim of LHCf is to provide a crucial calibration on the existing interaction models used in high energy cosmic ray simulations. To achieve that, LHCf measures neutral particles emitted in the very forward region from the LHC interaction point. LHCf has two independent detectors named Arm1 and Arm2. Each detector is installed on each side of the interaction point at a distance of 140m and is packed in an aluminium box of $90\text{ mm}^w \times 620\text{ mm}^h \times 290\text{ mm}^l$ that fits to the massive zero degree neutral absorbers (Target Neutral Absorber, TAN) instrumentation

slot. Each detector is compact, and has two shower sampling calorimeters with four position sensitive layers (each calorimeter is called “tower”). The cross section size of the towers are $20\text{ mm} \times 20\text{ mm}$ and $40\text{ mm} \times 40\text{ mm}$ for Arm1 and $25\text{ mm} \times 25\text{ mm}$ and $32\text{ mm} \times 32\text{ mm}$ for Arm2. Towers are composed of 22 tungsten plates and 16 plastic scintillators. The total thickness is 44 radiation lengths. For the position sensitive layers, Arm1 uses SciFis and Arm2 uses silicon micro-strips sensors. The structure of the current Arm1 calorimeter is shown in Fig.1 and a picture of a SciFi belt is shown in Fig.2. This two calorimeters structure allows us to reconstruct π^0 decaying into a γ pair. By measuring the energy and position of these γ 's, the energy and momentum of the initial π^0 produced by proton-proton collisions at the interaction point can be derived. The first

phase of the LHCf experiment has been achieved in July 2010 and 110 million shower events have been collected at $\sqrt{s} = 7$ TeV collision. The detectors is now removed from the LHC tunnel.

For the coming $\sqrt{s} = 14$ TeV collision run, an upgrade of the detector is necessary to cope with the possible radiation damage and the cerium (Ce^{+3}) doped gadolinium oxy-orthosilicate (Gd_2SiO_5 or simply GSO) scintillator [2] has been selected. The radiation hardness was evaluated and the results are presented in the reference. [3]. All plastic scintillators will be replaced by GSO scintillators [4]. For the position sensitive detector of Arm1, very small GSO scintillators (GSO bars) are manufactured to replace the SciFis. Such small GSO scintillators have never been used before. We used a ^{12}C beam of 290 MeV/n at HIMAC (Heavy Ion Medical Accelerator in Chiba) to investigate basic characteristics of GSO bars such as the position dependence of the light yield and cross talk between bars.

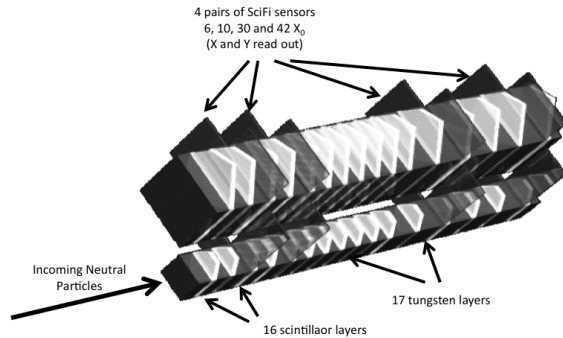


Figure 1: Schematic drawing of the current LHCf Arm1 detector [1]. The two towers are 240 mm long, and have transverse dimension of 20 mm \times 20 mm (small tower) and 40 mm \times 40 mm (large tower).

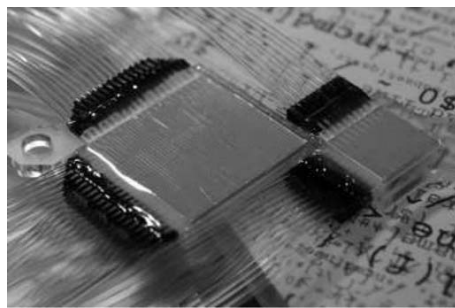


Figure 2: Picture of a SciFi hodoscope glued on the acrylic frame. Left and right parts are single hodoscope planes of the small and large tower calorimeters, respectively.

2 The LHCf GSO bar position sensitive detector and the prototype

The position sensitive layer of the upgraded Arm1 detector will consist of 4 X-Y pairs of GSO bundle hodoscopes placed at depths of 6, 10, 30 and 42 X_0 . Like the current detector, they will have 20 and 40 GSO bars of 1 mm \times 1 mm square cross section for the small and large tower, respectively (See Fig.3). Each GSO bar will be glued to a silica-fused fiber (Polymicro FVP-600-660-710) of 710 μm in radius (core 600 μm in radius) and guided to a multi-anodes photomultiplier (MAPMT, Hamamatsu Ultra bialkali H7546). LHCf measures showers with energy of a several tens GeV to 7 TeV and a large dynamic range is required. By reducing the number of dynodes from 12 to 8, MAPMT's gain decreases without changing its high voltage. Each MAPMT are composed of 64 anodes and are connected to 60 (=20(small)+40(large)) fibers from a GSO bundle X or Y layer. In total, 8 MAPMTs are used to read out all 480 fibers.

The signals of MAPMT are read out with a front-end circuit (FEC). The FEC packed a 16 bit ADC for each VA chip (VA32HDR14) and an FPGA for the trigger logic. The schematic diagram of the FEC and the DAQ system is shown in Fig.4. One FEC is composed of two units. After the sample & hold, the 32 signals from the MAPMT are multiplexed in each chip and converted to 16-bit ADC. With the trigger condition defined with the FPGA, the data are transferred to the VME DAQ system. The FEC also supplies the high voltage to the MAPMT. As shown in Fig.4, an FEC is made of four units that contain two identical sets of circuit for 32 channels each on the front and back sides ($32 \times 2 = 64$). The DAQ time for one event is less than 100 μs . But there is a pile-up problem. Since the VA32HDR14 needs 2 μs to complete the shaping and sample and hold process, the interval of two successive events must be less than 2 μs . A low luminosity run is required to record most of the events for the coming operation at $\sqrt{s}=14$ TeV run.

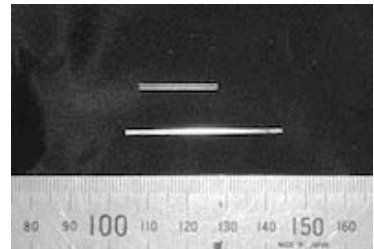


Figure 3: Picture of GSO bars. They have 1 mm \times 1 mm square cross section, 20 mm and 40 mm length for small tower and large tower, respectively.

A protote of a GSO bundle which consists of 5 pieces of 40 mm-long GSO bars glued to 350 mm long silica fuzed fiber has been manufactured. The MIP (Minimum Ionizing Particle) has been measured by observing cosmic ray muon

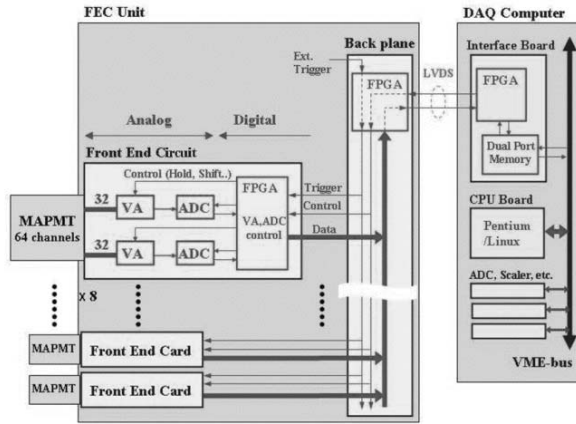


Figure 4: Schematic diagram of the FEC and DAQ for the position sensitive detector.

(see Fig.5). The MAPMT is used in a high gain mode. To obtain the MIP peak, the ADC distribution is fitted with a convoluted function of Landau and Gaussian distribution. The peak corresponds to 3-4 photoelectrons which is 50% of the current SciFi's MIP peak.

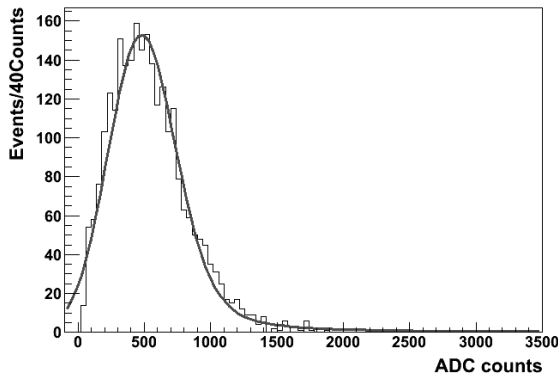


Figure 5: The ADC distribution of GSO bar for cosmic ray muon. The Fitting is done with a convoluted function of Landau and Gaussian distribution. The peak value corresponds to 3-4 p.e.

3 Experiment at HIMAC

Since the GSO bars are very small, their performance had to be evaluated with accelerators. Using ^{12}C (290 MeV/u) beam at HIMAC, large signals and accurate measurements are expected.

3.1 Experimental set up

Two sets of GSO bundle have been tested at HIMAC. One is composed of GSO bars without reflector (hereafter “air gapped”). The high refractive index (1.85 at $\lambda=450\text{nm}$) of the GSO leads to a small critical angle with air, thus the best reflectivity is expected. The other is painted with a white acrylic paint (hereafter “painted”) to avoid cross talk between GSO bars. The experimental setup is shown in Fig.6. Two fixed trigger scintillators (10 mm \times 10 mm \times 2 mm) are put at the upstream position of the beam line and the GSO bundles are set on a movable table.

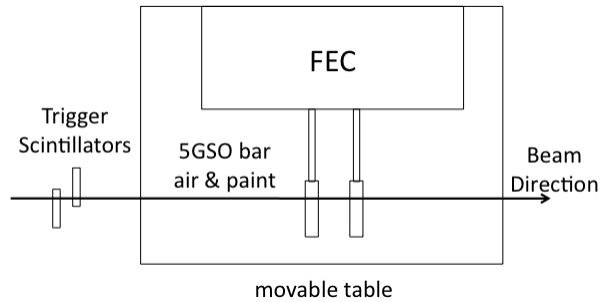


Figure 6: The experimental setup at HIMAC. The trigger scintillators were fixed and GSO bundles were put on a movable table.

3.2 The position dependence of light yield

Uniformity of scintillators is important to ensure the performance of a position sensitive detector. The response of each bar is measured by injecting the beam every 5 mm from the edge of the bars. The ADC peak to the C beam is fitted with a Gaussian distribution and each peak value is normalized with the peak value when the beam is injected in the center of the corresponding bar. As shown in Fig.7, the position dependence of the light yield is about $\pm 15\%$ for air gapped GSO bars (Fig.7, top) and -10% to +30% for painted GSO bar (Fig.7, bottom). The position dependence is worse for painted bars than air gapped bars because of the reflectivity of the acrylic paint which is not enough large. A large fluctuation between painted bars is observed. The position dependence should be as small as possible, so the air gapped bar is favored for LHCf. For the air gapped bar, the effective attenuation length of scintillating photon is 150 mm. The attenuation is not negligible and this effect will have to be taken into account for analysis.

3.3 Estimation of cross talk between GSO bars

If the GSO bars are to be used without reflector, the cross talk between bars should be estimated. Cross talk occurs when a scintillating photon escapes from a bar and enters into another where it is absorbed and re-emitted.

For each event, the bar which is hit by the beam is selected

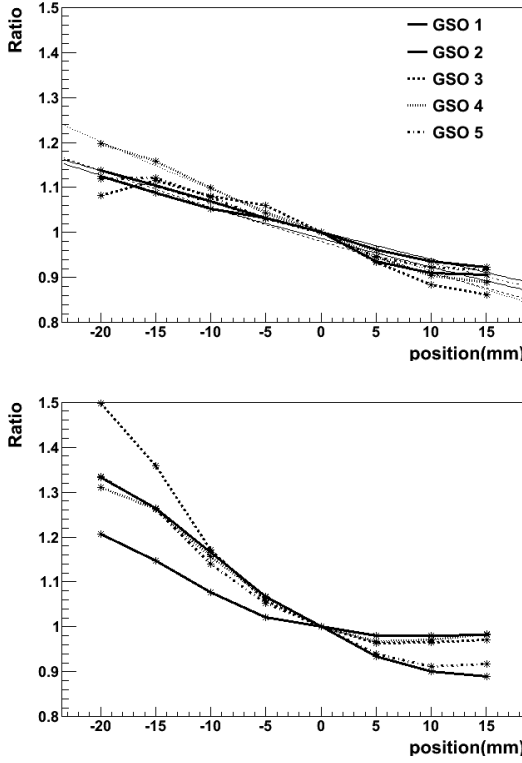


Figure 7: Position dependence of light yield for air gapped GSO bars (top) and painted GSO bars (bottom). The horizontal axis is the position of the beam (0 mm is the center of GSO bar) and the vertical axis is the ratio between the value when the beam was injected in the center of the bar. For air gapped GSO bar, the results are fitted with a exponential function and gives an effective attenuation of 150 mm.

and the response of the neighboring bars are observed. This procedure is applied for all runs and all GSO bars. The relative signal size with respect to the signal size found in the hit bar is plotted in Fig.8 as a function of distance from the hit bar. The effect of cross talk is about 8% for neighboring GSO bar and 1% for the next one. The LHCf will measure shower particles, thus these effects are expected to be not critical. As a result, the air gapped GSO bars are expected to give better result.

4 Summary

The basic properties of GSO bar have been investigated at HIMAC. The air gapped GSO bar gives a better performance than painted bar. For the air gapped bar, cross talk between bars is present. The performance using air gapped GSO bar will be simulated with EPICS simulation code [5]. The position dependence and cross talk effect will be included. The results will be presented at the conference.

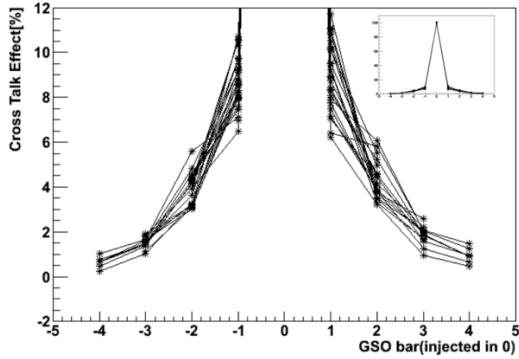


Figure 8: Cross talk between GSO bars. GSO bar hit by the beam was labeled 0. The neighboring bars on each was labeled in sequence. The values are normalized according to its own C peak value. The figure is zoomed and the overall distribution is shown in the top right figure.

References

- [1] O. Adriani *et al.*, JINST, 2008, **3**: S08006
- [2] K. Takagi and T. Fukazawa, Appl. Phys. Lett. **42** (1983) 43-45
- [3] M. Tanaka *et al.*, Nucl. Instr. and Meth. **A 404** (1998) 283-294
- [4] K. Kawade *et al.*, Proc. 32th ICRC (2011)
- [5] K. Kasahara, EPICS Homepage, <http://cosmos.n. kanagawa-u.ac.jp>